ELSEVIER

Journal of Nuclear Materials 313–316 (2003) 754–758

journal of nuclear materials

www.elsevier.com/locate/jnucmat

Experimental investigations on hydrocarbon-enhanced MAR processes in low temperature plasma in divertor simulator MAP-II

S. Kado [a,*], H. Kobayashi [b], T. Oishi [b], S. Tanaka [b]

[a] *High Temperature Plasma Center, The University of Tokyo, 2-11-16 Yayoi, Bunkyo-ku, Tokyo 113-8656, Japan*
[b] *Department of Quantum Engineering and Systems Science, Graduate School of Engineering, The University of Tokyo, 7-3-1 Hongo, Bunkyo-ku, Tokyo 113-8656, Japan*

Abstract

Plasma recombination phenomena were observed in the interactions of hydrogen or hydrocarbon gasses with low temperature helium plasma stream along the longitudinal magnetic field, which simulated the divertor region. The reduction of the ion saturation current implies the existence of molecular activated/assisted recombination (MAR) processes. The recombination efficiency is much stronger in the methane and ethane than in the hydrogen injection case, namely, $He \ll H_2 \ll CH_4 < C_2H_6$. In order to clarify the dominant processes in the hydrocarbon-enhanced MAR phenomena, spectroscopy on the $A^2\Delta$–$X^2\Pi$ band of CH radical was conducted. In the electron temperature lower than about 6 eV, the dominant dissociation and emission processes of the CH radicals have qualitatively been revealed to be related to their charge exchange with bulk ions, which can be followed by the dissociative recombination with electrons.

Keywords: Hydrocarbon; MAR; Detachment; CH band; Change exchange; Dissociative; Recombination

1. Introduction

Volumetric recombination processes in experimental fusion edge plasmas have been recognized as being relevant to plasma detachment phenomena, which drastically reduce particle and heat fluxes to the wall [1]. Atomic and molecular processes, which play a crucial role in achieving the detached condition, have been studied comprehensively in linear divertor simulators [2,3]. Conventional electron-ion recombination (EIR) for high density ($\gg 10^{13}$ cm^{-3}) cold ($\ll 1$ eV) plasma and recently recognized molecular activated/assisted recombination (MAR) associated with vibrationally excited hydrogen molecules in higher temperature (<2–3 eV) are regarded as the main mechanisms [4]. Recently, Janev et al. predicted that the ionization of hydrocarbon molecules C_xH_y due to charge exchange with bulk ions leads to an enhanced dissociative recombination with electrons in a higher temperature regime (<8 eV) [5]. This could be another type of MAR process and expand the operation temperature window for divertor detachment up to around 8 eV. The condition, under which this hydrocarbon MAR is responsible, is that the charge exchange ionization of hydrocarbon radicals should be more frequent than the electron impact ionization, since the latter cannot drastically enhance the recombination other than lowering the electron temperature, while the former can act as a catalysis to transfer more electrons to bulk ions throughout the dissociative recombination cycles of the hydrocarbon radicals.

For the purpose of identifying the dissociation processes of hydrocarbon radicals, intensities of the CH band spectra, mostly radiative transition $A^2\Delta$–$X^2\Pi$

* Corresponding author. Tel.: +81-3 5841 7667; fax: +81-3 5802 7221.
E-mail address: kado@q.t.u-tokyo.ac.jp (S. Kado).

0022-3115/03/$ - see front matter
PII: S0022-3115(02)01420-4

around 430 nm, can be used together with some dissociation and emission models.

This paper studies the MAR phenomena observed in a variety of gas injection experiments in the helium discharges. After a brief description on the experimental setup in Section 2, the decay of the ion saturation current along the plasma column and its dependence on the neutral pressure are investigated with the injection of methane (CH_4) and ethane (C_2H_6), in Section 3. The comparison with the helium (H_e) or hydrogen (H_2) injection case is provided. In Section 4, the CH band emission is measured and compared with the calculations using two major dissociation and emission models, charge exchange and electron impact chains. Finally, the main conclusions are summarized in Section 5.

2. Experimental setup

The diagnostics as well as the target chamber of the divertor/edge plasma simulator, MAP-II (Material and Plasma), is schematically shown in Fig. 1. Plasma stream with a diameter of about 5 cm along a longitudinal magnetic field of about 0.02 T are generated in an arc source region between a flat LaB_6 cathode plate and an anode pipe. The plasmas are transmitted to a gas target chamber at a distance of 1.5 m from the plasma source and finally terminated at the floating target plate. Although a differential pumping system enables a good pressure isolation between the source chamber and the target chamber connected with a drift tube [6], the gate valve on the former, GV1, was closed to lower the electron temperature at the entrance of the target chamber for the detachment experiments. In contrast, with GV1 open, the electron temperature T_e as well as the electron density n_e can be controlled over a wider range by an additional helium puff into the target chamber. This option is suitable for the spectroscopic study.

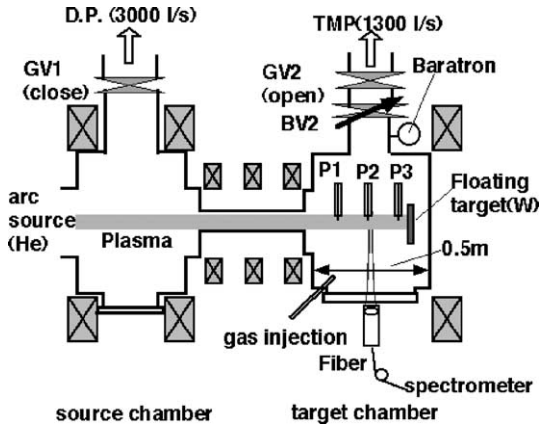

Fig. 1. Schematic view of the vacuum chamber and the diagnostic system of the MAP-II device.

The Langmuir probe system consists of three tungsten electrodes located at distances of 5, 25 and 35 cm from the entrance of the target chamber, which referred to P1 (upstream), P2 (midstream) and P3 (downstream), respectively. The probe electrodes were often cleaned by both positive and negative biasing with hydrogen puffing to avoid contaminations by hydrocarbon radicals. For spectroscopy, a 1 m Czerny-Turner monochromator with a 1200 graves/mm grating equipped with a photo-multiplier tube was used. The wavelength resolution is about 0.042 nm at 50 μm slit width. An object lens collects light from the line-of sight across the plasma stream focusing on the region 2 mm in diameter where the probe P2 is located.

3. Rapid decay in the ion flux by molecular gas injections

In this study, a discharge voltage and current were set to 70 V and 45 A, respectively. Operations with GV1 closed were applied to achieve low temperature experiments for the MAR studies in the helium plasma stream. Firstly, the evolution of n_e and T_e as increasing helium gas pressure in the target chamber is shown in Fig. 2(a) and (b) as a reference for the different gas puffing experiments. The helium base pressure without additional gas puff was 6.3 mTorr, yielding T_e at P1 about 4 eV. With additional helium puffing to 22 mTorr, T_e at P1 can be even lowered to 2 eV. A small increase in n_e at P1 can be seen in the first half of the pressure scan in which slightly more ionization occurs in the target chamber as the base pressure increases. Moderate decays in n_e along the column are mainly due to the radial diffusion and may partly be due to the EIR in the cold peripheral region, while that in T_e due to the electron-ion and electron-neutral inelastic collisions.

When the molecular hydrogen is puffed in the target chamber, however, the pressure dependences of n_e and T_e are different as shown in Fig. 2(c) and (d), respectively. Because of the higher ionization rate than that of helium, n_e increases while T_e decreases as the pressure increases below 8 mTorr. On the other hand, both n_e and T_e at P1 and P2 rapidly decrease when the neutral pressure increases in the range from 8 to 14 mTorr. Because the radial diffusion behavior in the cases of small amount of hydrogen additional injection may not be much different from that in the pure helium case, this n_e reduction can be explained by so-called volumetric recombination induced by hydrogen molecules, namely the MAR processes. The fact that the MAR rate exceeds the ionization rate at about 2 eV may contribute to the rollover in the n_e evolutions.

As seen in Fig. 2(d), T_e values at P1, P2 and P3 begin to increase again when they become close to about 1 eV.

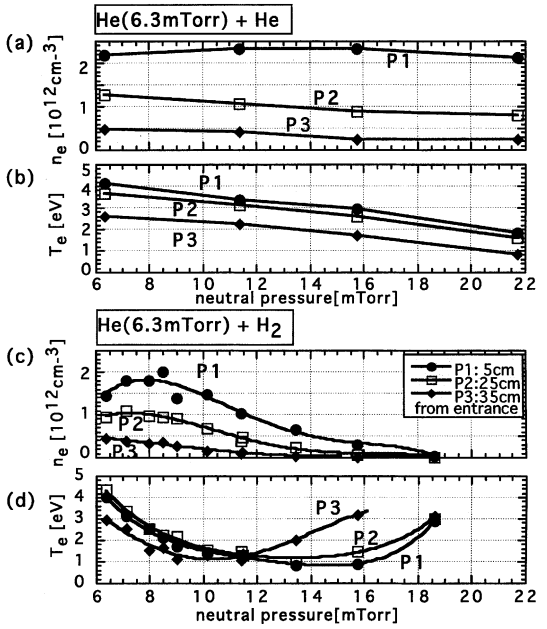

Fig. 2. Evolution of the electron density n_e (a) and temperature T_e (b) as a function of neutral gas pressure for the He puff case. (c) and (d) are for H_2 puff cases.

However, there is no apparent physical mechanism to increase T_e, because the plasma discharge region, in which electrons are accelerated by a discharge voltage, is far from the target chamber and the source condition is not much changed by varying the pressure in the target chamber. This unphysically high T_e evaluation is caused by the distorted single probe I–V characteristics, namely, the decrease of the electron saturation current as neutral pressure increases. This anomaly in single probe characteristics has widely been reported in the recombining (EIR and MAR) plasmas both in divertors [7] and in divertor simulators [8], which is considered due to the plasma impedance between a probe tip and a reference electrode, and/or by fluctuating space potential [9]. Thus, we intrinsically regarded that this anomaly could be a symptom of MAR since plasma parameters in this experiment is far beyond EIR to be effective.

Therefore, for the purpose of investigating the MAR phenomena, quantitative comparisons as to n_e or T_e measured with single probes are sometimes impossible. Rather, a relative change of the ion saturation current, namely ion flux, is supposed to be more desirable to give a comparison of various gas species on the effect of enhanced plasma recombination.

The relative change of the ion saturation current as a function of the neutral pressure with puffing of helium (a), hydrogen (b), methane (c) and ethane (d) gasses is shown in Fig. 3. The initial value mainly corresponds to the decay in relation to inelastic collisions and the diffusion effect between P1 and P2 or P3. Thus, the dependence of the ratio P2/P1 and P3/P1 on the neutral pressure mainly indicates momentum loss mechanisms. As seen in this figure, the relative reduction of the ion flux can be described in an exponential decay form, and strongly depends on the type of puffing gas. The e-folding pressure for (P2/P1, P3/P1) can be deduced as (44.8, 37.8), (13.2, 8.8), (2.3, 1.4) and (1.6, 0.4) mTorr for He, H_2, CH_4 and C_2H_6, respectively. Similar to the observations in several divertor simulators, the decay in the ion flux by a hydrogen puff can be explained by the hydrogen MAR.

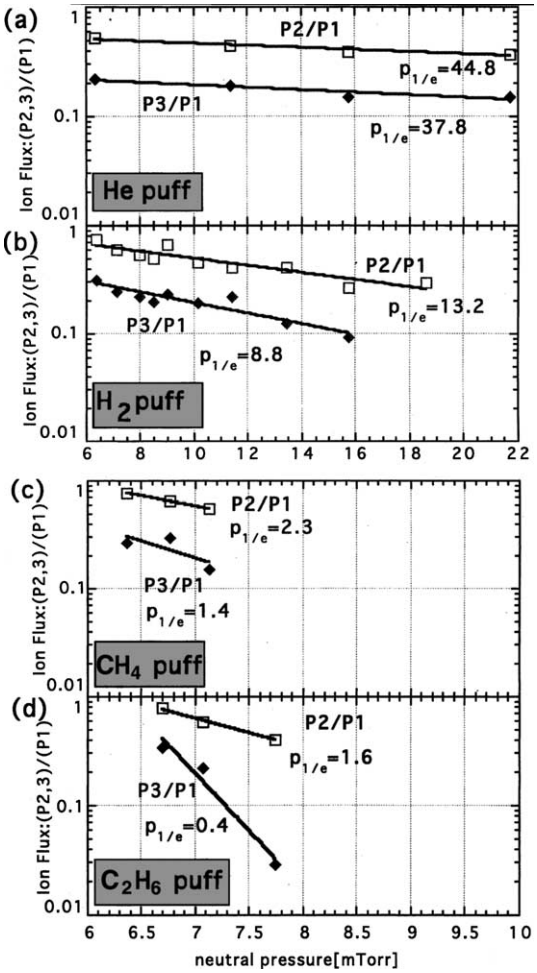

Fig. 3. Evolution of the ion saturation current at P2 (midstream) and P3 (downstream), normalized to P1 (upstream), as a function of neutral pressure for (a) He, (b) H_2, (c) CH_4 and (d) C_2H_6 puffing series. The values of $P_{1/e}$ denote the e-folding pressures in mTorr. Note that the pressure scale of (c) and (d) is expanded compared with that of (a) and (b).

However, much more rapid decay observed in CH_4 and C_2H_6 puffs could imply the existence of the stronger plasma recombination enhanced by hydrocarbons.

According to Janev's calculations, 9.3% and 3.7% of CH_4 and C_2H_6 concentrations, respectively provide the same MAR effects as H_2 at $T_e = 1$ eV [5]. Although the differences in the working gas, ambiguity in T_e, transport effects and other atomic and molecular processes as well as experimental errors should be taken into account for the integrative quantitative evaluations, the observed e-folding pressures demonstrate at least a qualitative tendency of the dependence of the recombination efficiencies on the type of molecular gasses.

Inspired by these observations, a spectroscopic measurement is performed to confirm if the charge exchange ionization of hydrocarbon molecules with bulk ions exceeded the electron impact processes in dissociation cycles in this temperature regime.

4. Dominance of CX-DR in low temperature plasma with hydrocarbon

Hydrocarbon MAR should be initiated from a charge exchange, $He^+ + C_xH_y \rightarrow He + C_xH_y^+$, and it is followed by a dissociative recombination, $e + C_xH_y^+ \rightarrow \sum_{k,l} C_{x-k}H_{y-l} + H$. Thus, parametric dependence of the CH band emission, $A^2\Delta$–$X^2\Pi$, was investigated to find out experimentally the possibility of the process, shown in Fig. 4. Background pressure is about 2 mTorr with GV1 open, and is increased up to 10 mTorr by an additional helium puff corresponding to the T_e range from about 10–4 eV, respectively. Partial pressure of C_2H_6 was fixed at only 0.15 mTorr to minimize the influence of C_2H_6 on the plasma conditions. The discharge current was set to be 30 A. The rotational structure of the electronic state CH(A) is often characterized by the rotational temperature T_{rot}. The rotational distributions having rotational quantum numbers K from 2 to 15 in CH(A) with the vibrational ground state are deduced from the well separated P-branch spectra, and Q- and R-branch spectra are reconstructed to check if they reproduce the observed Q- and R-branches, since there are some lines in P branch which are contaminated by the other spectra. It was observed that the rotational distribution could often be described in bi-Maxwellian form at T_{rot}'s of about 3000–5000 and 800–1500 K. Thus, the total CH band emission is determined from the photon flux expected from a best fit in either Maxwellian or bi-Maxwellian rotational distribution. Note that the objective in this study is to clarify if there is a dominant dissociation process to a lowest order, and not to determine the hydrocarbon radical fractions or kinetics. Therefore, for the data which are not available, the 'shape' of dependence of rate coefficients on T_e is alternatively used, especially in the process related to C_2H_m ($m < 6$). Data for electron impact processes was taken from Ref. [10] and for charge exchange from Ref. [1]. The charge exchange rates of H^+ and He^+ with ethane as a function of velocity were assumed to be the same. By varying the residence time of radicals and the ambipolar diffusion time of ions from 1/3 to 3 of the simple estimations, the sensitivity to the calculated photon flux was checked and confirmed that the dependence on the parameters remained similar.

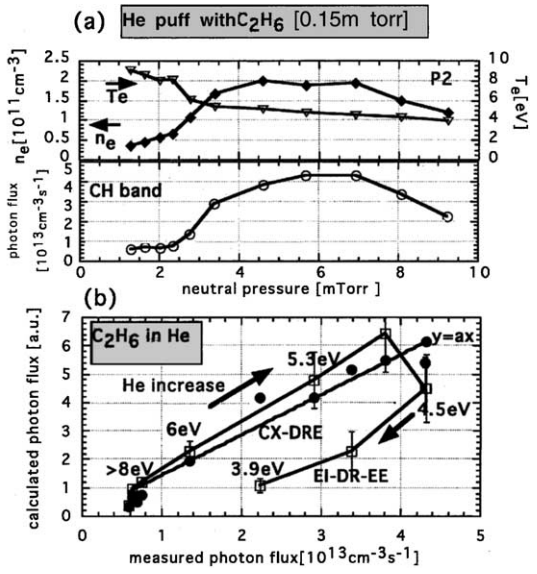

Fig. 4. (a) Evolution of the n_e, T_e and CH band emission as a function of the helium pressure. (b) Comparison of the calculated CH band emission with the measured value. The parameters in (a) are applied to two major models, CX-DRE (filled circle) and EI-DR-EE (open square). Hysteresis seen in the EI-DR-EE plot shows the discrepancy of the model used in the calculation.

Fig. 4(a) shows the evolutions of the plasma parameters at P2 together with that of the line-integrated A–X emission intensity at the same location as a function of the helium pressure. Fig. 4(b) gives the comparison of the total emission intensities obtained from experiments with the modeled emissions from EI-DR-EE only and CX-DRE only for the same plasma parameters obtained in Fig. 4(a). CX-DRE represents the CX-DR chain to form an exited state CH(A) while EI-DR-EE represents the electron impact ionization (EI) chain followed by a dissociative recombination (DR) to form a ground state CH(X), then electron impact excitation (EE) to a CH(A). Since the concentration is paid on the parametric dependence of relative emission intensities in the modeling rather than of the absolute values, the emissions in the experiments as a function of those from the modeling should be linear in any plasma parameters if either EI-DR-EE or CX-DRE is dominant. The linearity can be seen from CX-DRE when T_e is lower than 6–8 eV while no linearity can be found from EI-DR-EE in Fig. 4(b). This suggests that CX-DRE can

be one of the dominant processes contributing to CH(A)–CH(X) emission.

Although one may think that there are plenty of dissociation-emission paths, the dependences of the dissociation-relevant reaction rate on n_e and T_e may generally be categorized by these two major processes, electron impact (EI) and charge exchange (CX). For example, since the T_e dependences of reaction rate for electron impact ionization (EI) and dissociation (ED) are similar, the results are not much different even the electron impact dissociation processes occurs in the EI-DR chain. Therefore, the process which triggers the dissociation chain can be dominant. One can also speculate from the Fig. 4(b) that the deviation from linearity in the CX-DRE model is mainly in the regime where T_e is higher than 8 eV. Namely, it can be said that the CX-DR process plays a significant role in the dissociation processes below 6–8 eV. It is also true for the methane case [11].

5. Summary and conclusions

Strong reduction of the ion flux was observed in helium plasma discharges with additional gas puffing of hydrogen, methane, ethane and helium as a comparison. The hydrogen MAR phenomenon clearly appears when T_e becomes lower than 2 eV. In the hydrocarbon case, qualitative observations suggest the evidence of the hydrocarbon-enhanced MAR processes from the following facts:

(1) The reduction efficiency of the ion flux is $He \ll H_2 \ll CH_4 < C_2H_6$. This tendency qualitatively agrees with the theoretical value.
(2) T_e without gas puff, 4 eV, is already in the region where hydrocarbon MAR is expected to occur.
(3) It was strongly indicated that the CX-DR process dominates the CH band emission below 6 eV.

However, the number of measurements is limited in this work and a more quantitative approach, including diffusion kinetics, might be important. Also, C_3H_8 or C_4H_{10} injection experiment may give more information on the evidence of the hydrocarbon MAR processes and on the divertor detachment scenario in fusion reactors. These are the subjects of research for the near future.

Acknowledgements

One of the authors (S.K.) wishes to thank Dr R. Janev and Dr B. Xiao for their useful comments. He also thanks the referees for their help in improving this paper. This work was partly supported by TEPCO Research Foundation.

References

[1] S.I. Krasheninnikov, A. Yu Pigarov, D.J. Sigmar, Phys. Lett. A 214 (1996) 285.
[2] N. Ohno et al., Phys. Rev. Lett. 27 (1998) 818.
[3] M.G. Rusbridge et al., Plasma Phys. Control. Fusion 42 (2000) 579.
[4] S.I. Krasheninnikov et al., Phys. Plasmas 4 (1997) 1638.
[5] R.K. Janev, T. Kato, J.G. Wang, Phys. Plasmas 7 (2000) 4364.
[6] K. Kobayashi, S. Kado, B. Xiao, S. Tanaka, J. Nucl. Mater 290–293 (2001) 648.
[7] R.D. Monk et al., J. Nucl. Mater. 241–243 (1997) 396.
[8] N. Ezumi et al., Contrib. Plasma Phys. 38 (1998) 31.
[9] N. Ohno et al., Contrib. Plasma Phys. 41 (2001) 473.
[10] H. Tawara et al., NIFS-DATA-6, Nagoya, Japan, 1990.
[11] H. Kobayashi, S. Kado, B. Xiao, S. Tanaka, Jpn. J. Appl. Phys., accepted for publication.